An X-Ray Investigation of the Structures of the Tetrachloro- and Tetrabromoaurate(III) Ions in Aqueous Solution

Masunobu MAEDA, Hitoshi OHTAKI, and Georg JOHANSSON*

Department of Electrochemistry, Tokyo Institute of Technology, O-okayama, Meguro-ku, Tokyo 152
**Department of Inorganic Chemistry, Royal Institute of Technology, S-100 44 Stockholm 70, Sweden*

(Received May 25, 1974)

The structures of the $AuCl_4^-$ and the $AuBr_4^-$ complexes in aqueous solutions have been determined from X-ray scattering measurements on concentrated solutions of tetrachloroauric and tetrabromoauric acids. Both the tetrachloroaurate(III) and the tetrabromoaurate(III) complexes were found to have a square planar symmetry. The values obtained for the interatomic distances within the complexes are: Au–Cl, 2.29_1 Å; *cis*-Cl–Cl, 3.24 Å; *trans*-Cl–Cl, 4.58 Å; Au–Br, 2.43_2 Å; *cis*-Br–Br, 3.44 Å; *trans*-Br–Br, 4.86 Å.

Gold(III) is known to combine with chloride, bromide and iodide ions to form stable complexes of the type AuX_4^- in acid solutions.[1] A square planar model for the structures of the $AuCl_4^-$ and the $AuBr_4^-$ ions in aqueous solutions has been found to be consistent with Raman spectroscopic measurements.[2] In the solid state the $AuCl_4^-$ and the $AuBr_4^-$ complexes have been shown by X-ray scattering,[3-6] Raman and IR measurements[7,8] to have a square planar structure.

As a preliminary to an investigation of the structures of the mixed halide complexes of gold(III) in aqueous solutions more detailed information was needed on the structures of the $AuCl_4^-$ and the $AuBr_4^-$ complexes in solution. For this purpose X-ray scattering measurements have been carried out on concentrated auric chloride and bromide solutions containing the $AuCl_4^-$ and the $AuBr_4^-$ complexes.

Experimental

Preparation and Analysis of Sample Solutions. A solution of tetrachloroauric acid was prepared by dissolving metallic gold of 99.99% purity in *aqua regia* and removing the nitric acid by repeated evaporation with hydrochloric acid.

Gold was determined gravimetrically as metallic gold after reduction with hydrazine sulphate. Chloride was determined gravimetrically as AgCl after reduction of the gold with hydrazine sulphate. The hydrogen-ion concentration was calculated from the relation $[H^+]=[Cl^-]-3[Au^{3+}]$.

A solution of tetrabromoauric acid was prepared by dissolving metallic gold in a mixture of hydrobromic acid and hydrogen peroxide. The analysis of the solution was made by the same procedure as used for the tetrachloroauric acid solution.

The density of a solution was determined with a pycnometer.

The compositions of the solutions investigated are given in Table 1.

TABLE 1. COMPOSITIONS OF THE SOLUTIONS (in g-atom·l^{-1})

	Tetrachloroaurate soln.	Tetrabromoaurate soln.
Au	3.133	2.766
Br	—	12.78
Cl	13.61	—
O	38.78	36.76
H	81.77	77.99

X-Ray Scattering Measurements. The diffractometer used was the same as that described in a previous paper.[9] Mo$K\alpha$ radiation ($\lambda=0.7107$ Å) was used for the measurements. The slit-openings were 1/12°, 1/4° and 1°. A LiF focusing monochromator was placed between the receiving slit and the scintillation counter. Further monochromatization was obtained by means of a pulse-height discriminator. The scattered intensity was measured at discrete points between $\theta=1°$ and 70°, where 2θ is the scattering angle. Points were taken at angular steps of 0.1° in θ up to $\theta=20°$, and 0.25° to $\theta=70°$. The number of counts collected at each angle corresponded to a standard deviation in the measured intensities of about 0.3%. To check long-time variations in the measured intensity, the measurements at each slit combination were made repeatedly. For each slit-opening the measured intensities after corrections for background radiation (about 0.90 counts per second) were recalculated to a common slit width through the use of measurements in overlapping regions. The amount of incoherent radiation passing through the monochromator was estimated from the spectrum of the X-ray tube and the resolving power of the monochromator as described previously.[9,10] It was also estimated experimentally by comparing, at a high angle ($\theta=65°$), intensity measurements obtained when a zirconium filter was placed between the tube and the sample with corresponding measurements with the same filter placed between the sample and the scintillation counter.

All measurements were carried out in a room thermostated at 25±2 °C.

Treatment of Intensity Data

The measured intensities were corrected for polarization in the sample and in the monochromator, and were normalized to correspond to the sum of the calculated coherent and incoherent scattering in the high-angle region ($\theta \gtrsim 50°$) for a unit of volume of solution containing one gold atom. The normalization factors calculated in this way agreed within less than 1% with those calculated by the method of Norman[11] and Krogh-Moe.[12]

The scattering factors used for Au, Br, Cl, and O were those given by Cromer and Waber.[13] For H the values given by Stewart *et al.*[14] were used. Values for the incoherent scattering were those given by Cromer and Mann[15] for Au, by Cromer[16] for Br, Cl, and O, and by Compton and Allison[17] for H. The incoherent scattering was corrected for the Breit-Dirac factor.

Anomalous dispersion corrections were taken from Cromer and Liberman's paper.[18]

TABLE 2. OBSERVED INTENSITY VALUES AS A FUNCTION OF $s=4\pi \sin\theta/\lambda$.
$I(s)$=observed intensities after normalization, $i(s)$=reduced intensities (corrected for low-frequency additions to the intensity curves).

1) Tetrachloroaurate System

s	$I(s)$	$i(s)$	s	$I(s)$	$i(s)$	s	$I(s)$	$i(s)$
0.401	5958	−2058.0	2.339	4833	−783.9	4.248	3362	−84.8
0.432	6279	−1721.3	2.369	4849	−724.5	4.278	3322	−100.5
0.463	6580	−1404.4	2.400	4868	−662.7	4.308	3296	−103.5
0.494	6854	−1112.4	2.430	4884	−602.9	4.337	3253	−122.3
0.525	7156	−791.4	2.461	4907	−537.5	4.367	3212	−140.0
0.555	7350	−577.3	2.491	4925	−477.2	4.397	3170	−155.7
0.586	7501	−404.2	2.522	4947	−412.8	4.427	3132	−173.8
0.617	7481	−401.6	2.552	4963	−354.4	4.457	3112	−171.8
0.648	7607	−251.7	2.583	4987	−288.2	4.487	3065	−196.4
0.679	7497	−335.1	2.614	4999	−235.3	4.517	3032	−207.5
0.710	7467	−338.3	2.644	5015	−178.0	4.547	3001	−216.3
0.740	7378	−398.5	2.675	5053	−98.6	4.576	2966	−230.4
0.771	7281	−466.4	2.705	5013	−97.8	4.606	2940	−234.7
0.802	7233	−484.2	2.736	5022	−48.3	4.636	2920	−234.2
0.833	7125	−560.6	2.766	5012	−17.3	4.666	2887	−246.0
0.864	7102	−551.8	2.797	5016	26.4	4.695	2859	−253.9
0.895	6999	−621.2	2.827	5018	67.7	4.725	2825	−268.0
0.925	6889	−696.6	2.857	5009	98.0	4.755	2810	−262.9
0.956	6932	−619.1	2.888	4998	126.9	4.785	2786	−266.8
0.987	6856	−659.4	2.918	4998	165.0	4.814	2761	−272.3
1.018	6769	−710.3	2.949	4986	191.5	4.844	2744	−269.8
1.049	6697	−745.1	2.979	4964	207.8	4.874	2721	−273.8
1.079	6637	−767.2	3.010	4973	254.7	4.903	2709	−267.7
1.110	6618	−747.8	3.040	4948	267.6	4.933	2681	−277.3
1.141	6599	−728.2	3.070	4945	301.7	4.963	2679	−260.2
1.172	6573	−713.9	3.101	4935	329.0	4.992	2657	−264.1
1.203	6555	−692.0	3.131	4936	366.1	5.022	2655	−248.4
1.233	6518	−687.9	3.162	4901	367.3	5.051	2647	−239.1
1.264	6501	−664.4	3.192	4911	413.1	5.081	2626	−242.5
1.295	6494	−630.4	3.222	4876	414.6	5.111	2624	−227.0
1.326	6478	−604.2	3.253	4861	434.8	5.140	2634	−200.1
1.357	6471	−569.6	3.283	4848	455.9	5.170	2617	−200.1
1.387	6441	−557.1	3.313	4841	483.7	5.199	2617	−182.8
1.418	6422	−533.9	3.344	4822	499.7	5.229	2609	−174.5
1.449	6392	−520.3	3.374	4782	493.8	5.258	2611	−155.8
1.480	6385	−483.9	3.404	4742	487.2	5.288	2612	−139.5
1.510	6335	−490.1	3.434	4697	475.2	5.317	2617	−118.0
1.541	6289	−492.3	3.465	4673	484.1	5.346	2615	−104.0
1.572	6202	−535.1	3.495	4621	465.0	5.376	2610	−93.5
1.603	6138	−555.4	3.525	4584	460.6	5.405	2618	−69.9
1.633	6055	−593.8	3.555	4529	437.7	5.435	2632	−40.8
1.664	5946	−657.6	3.586	4478	417.8	5.464	2620	−38.3
1.695	5833	−725.1	3.616	4430	400.8	5.493	2632	−11.0
1.725	5714	−799.2	3.646	4366	368.1	5.523	2643	15.2
1.756	5565	−902.8	3.676	4326	358.5	5.552	2648	34.9
1.787	5451	−971.4	3.706	4259	322.4	5.581	2651	52.5
1.818	5345	−1032.1	3.737	4200	293.4	5.610	2646	61.4
1.848	5256	−1076.4	3.767	4135	258.1	5.640	2658	87.2
1.879	5149	−1137.8	3.797	4081	233.5	5.669	2665	108.7
1.910	5101	−1140.1	3.827	4018	198.8	5.698	2655	112.1
1.940	5028	−1168.3	3.857	3970	180.2	5.727	2663	134.1
1.971	4966	−1185.1	3.887	3911	148.9	5.757	2663	147.6
2.002	4916	−1190.0	3.917	3863	128.8	5.786	2665	163.4
2.032	4864	−1196.9	3.947	3819	113.2	5.815	2641	152.5
2.063	4834	−1181.3	3.978	3774	94.6	5.844	1640	165.3
2.094	4808	−1162.7	4.008	3704	51.8	5.873	2640	178.1
2.124	4783	−1142.8	4.083	3671	46.0	5.902	2652	203.1
2.155	4787	−1094.6	4.068	3609	10.5	5.931	2634	197.6
2.185	4787	−1050.4	4.098	3578	4.9	5.960	2631	206.9
2.216	4801	−992.1	4.128	3526	−20.6	5.989	2620	208.4
2.247	4792	−956.7	4.158	3502	−20.1	6.018	2601	202.1
2.277	4793	−909.7	4.188	3452	−44.2	6.047	2613	226.8
2.308	4802	−858.6	4.218	3408	−63.5	6.149	2557	212.9

Table 2. (Continued)

s	$I(s)$	$i(s)$	s	$I(s)$	$i(s)$	s	$I(s)$	$i(s)$
6.221	2525	210.4	10.666	1113	−35.1	14.232	689	12.9
6.293	2481	194.6	10.727	1110	−26.8	14.278	686	14.6
6.365	2419	160.7	10.788	1110	−16.6	14.323	684	17.3
6.437	2355	148.8	10.848	1103	−13.3	14.368	678	15.7
6.509	2302	127.2	10.910	1093	−12.5	14.413	670	11.5
6.581	2220	102.8	10.971	1096	1.1	14.457	666	11.3
6.652	2172	76.7	11.031	1091	6.2	14.502	663	12.6
6.724	2105	49.8	11.091	1085	9.4	14.546	654	7.9
6.795	2079	19.8	11.151	1079	13.6	14.589	655	12.3
6.866	2029	−6.2	11.211	1071	14.9	14.633	650	11.0
6.937	1997	−30.6	11.271	1061	14.6	14.676	641	5.9
7.008	1965	−52.9	11.330	1062	24.5	14.719	639	7.8
7.079	1938	−69.4	11.389	1048	20.1	14.762	639	11.8
7.149	1904	−81.3	11.448	1042	22.8	14.804	636	12.7
7.220	1867	−95.5	11.507	1039	29.0	14.846	624	4.0
7.290	1841	−100.3	11.565	1028	27.0	14.888	624	8.0
7.361	1805	−114.8	11.623	1022	29.7	14.929	615	2.4
7.431	1777	−121.8	11.682	1007	23.2	14.970	610	0.5
7.501	1756	−121.5	11.739	999	24.4	15.011	607	0.7
7.570	1739	−118.3	11.797	998	30.9	15.052	604	1.2
7.640	1726	−110.9	11.854	982	23.8	15.092	600	1.1
7.710	1717	−100.8	11.911	972	22.0	15.132	595	−0.7
7.779	1705	−93.3	11.968	961	19.4	15.172	593	−0.2
7.848	1692	−86.7	12.025	950	15.9	15.212	588	−1.7
7.917	1687	−72.8	12.081	937	10.5	15.251	584	−2.9
7.986	1690	−51.0	12.138	932	13.2	15.290	582	−1.5
8.055	1679	−42.9	12.194	919	8.4	15.328	578	−2.9
8.123	1679	−25.0	12.294	908	5.1	15.367	573	−4.5
8.192	1680	−5.8	12.305	895	−0.6	15.405	572	−2.5
8.260	1669	1.0	12.360	886	−1.9	15.442	566	−5.1
8.328	1667	16.1	12.415	874	−6.7	15.480	564	−5.1
8.396	1665	31.2	12.470	870	−4.4	15.517	559	−7.0
8.464	1653	36.3	12.525	855	−11.7	15.554	556	−6.8
8.532	1647	47.4	12.579	852	−8.0	15.590	555	−5.7
8.599	1638	54.9	12.633	833	−19.5	15.626	550	−7.8
8.667	1624	57.9	12.687	827	−19.5	15.662	548	−7.2
8.734	1609	58.3	12.741	820	−19.9	15.698	539	−13.4
8.801	1589	54.8	12.794	811	−21.9	15.733	540	−10.0
8.868	1586	67.8	12.847	802	−24.8	15.768	541	−6.6
8.934	1563	60.1	12.900	798	−22.3	15.803	534	−10.6
9.001	1555	67.1	12.953	787	−26.4	15.838	531	−11.1
9.067	1527	54.7	13.005	782	−25.5	15.872	534	−6.2
9.133	1503	46.1	13.057	778	−22.9	15.906	531	−6.3
9.199	1484	41.2	13.109	771	−23.8	15.939	531	−3.9
9.265	1456	28.5	13.161	764	−24.6	15.972	527	−5.8
9.331	1438	24.6	13.212	761	−21.7	16.005	522	−8.7
9.396	1417	18.3	13.263	754	−23.7	16.038	522	−6.5
9.461	1403	18.7	13.314	751	−20.3	16.070	522	−3.9
9.526	1388	17.0	13.365	746	−19.9	16.102	520	−4.5
9.591	1354	−3.3	13.415	741	−18.8	16.134	519	−2.7
9.656	1338	−5.3	13.465	743	−11.2	16.166	519	−0.5
9.721	1311	−18.2	13.515	738	−11.3	16.197	514	−4.0
9.785	1295	−21.7	13.565	732	−11.3	16.227	516	0.1
9.849	1276	−27.4	13.614	732	−6.8	16.258	512	−1.6
9.913	1260	−30.5	13.663	718	−14.6	16.288	515	2.9
9.977	1245	−32.8	13.712	720	−8.5	16.318	508	−1.5
10.040	1230	−34.9	13.761	717	−5.4	16.348	509	1.3
10.104	1220	−32.3	13.809	718	0.2	16.377	509	2.6
10.167	1203	−37.2	13.857	715	2.6	16.406	506	2.0
10.230	1186	−42.0	13.905	714	6.5	16.434	501	−1.2
10.293	1180	−36.0	13.952	709	5.7	16.463	505	3.7
10.356	1164	−40.4	14.000	708	9.9	16.491	500	1.2
10.418	1156	−36.0	14.047	698	4.7	16.518	501	4.0
10.480	1143	−37.9	14.093	695	5.8	16.546	500	4.3
10.542	1132	−37.8	14.140	690	5.7	16.573	499	5.1
10.604	1123	−35.3	14.186	689	9.2			

Table 2. (Continued)

2) Tetrabromoaurate System

s	$I(s)$	$i(s)$	s	$I(s)$	$i(s)$	s	$I(s)$	$i(s)$
0.401	14224	1252.5	2.369	8493	−370.0	4.337	4840	−547.2
0.432	14159	1216.3	2.400	8470	−323.2	4.367	4737	−613.2
0.463	14276	1363.7	2.430	8423	−301.3	4.397	4662	−650.8
0.494	14255	1375.8	2.461	8369	−286.7	4.427	4605	−671.3
0.525	14134	1289.7	2.491	8359	−228.5	4.457	4519	−721.6
0.555	14092	1283.7	2.522	8300	−219.5	4.487	4454	−750.6
0.586	13967	1197.9	2.552	8249	−203.5	4.517	4403	−766.2
0.617	13775	1047.0	2.583	8224	−161.8	4.547	4327	−807.5
0.648	13703	1018.1	2.614	8215	−104.5	4.576	4286	−814.2
0.679	13430	791.5	2.644	8181	−73.0	4.606	4227	−838.6
0.710	13264	674.2	2.675	8209	20.8	4.636	4183	−849.6
0.740	13144	603.6	2.705	8131	7.2	4.666	4172	−826.9
0.771	12833	344.9	2.736	8123	64.0	4.695	4132	−834.3
0.802	12750	315.2	2.766	8079	84.2	4.725	4104	−829.3
0.833	12481	100.7	2.797	8072	140.7	4.755	4088	−813.3
0.864	12364	40.3	2.827	8091	222.5	4.785	4074	−795.7
0.895	12115	−150.3	2.857	8104	297.0	4.814	4062	−776.1
0.925	12004	−202.4	2.888	8098	352.7	4.844	4064	−743.7
0.956	11690	−454.5	2.918	8071	387.0	4.874	4042	−734.7
0.987	11451	−632.0	2.949	8113	489.5	4.903	4059	−687.1
1.018	11181	−838.3	2.979	8138	574.9	4.933	4093	−623.7
1.049	10880	−1073.7	3.010	8147	642.7	4.963	4097	−589.9
1.079	10560	−1328.1	3.040	8196	751.4	4.992	4116	−541.3
1.110	10307	−1513.5	3.070	8195	808.3	5.022	4165	−463.5
1.141	10043	−1709.7	3.101	8196	867.7	5.051	4177	−421.9
1.172	9783	−1901.4	3.131	8204	933.0	5.081	4230	−340.6
1.203	9480	−2133.7	3.162	8176	961.9	5.111	4269	−274.0
1.233	9202	−2342.0	3.192	8162	1004.2	5.140	4289	−225.8
1.264	8959	−2513.6	3.222	8141	1039.3	5.170	4322	−164.7
1.295	8706	−2696.1	3.253	8103	1056.7	5.199	4370	−89.5
1.326	8466	−2865.5	3.283	8040	1048.8	5.229	4401	−32.3
1.357	8272	−2981.5	3.313	7975	1037.5	5.258	4440	33.8
1.387	8048	−3140.2	3.344	7870	987.0	5.288	4504	124.7
1.418	7874	−3241.1	3.374	7800	970.4	5.317	4525	171.8
1.449	7729	−3314.1	3.434	7580	856.0	5.346	4578	251.1
1.480	7607	−3362.6	3.465	7493	820.7	5.376	4599	297.3
1.510	7475	−3421.7	3.495	7361	739.3	5.405	4622	345.9
1.541	7352	−3470.9	3.525	7269	698.4	5.435	4666	415.1
1.572	7302	−3448.2	3.555	7181	660.6	5.464	4684	458.3
1.603	7256	−3420.6	3.586	7094	623.6	5.493	4681	480.0
1.633	7224	−3378.5	3.616	6992	570.7	5.523	4705	529.1
1.664	7222	−3306.0	3.646	6869	496.8	5.552	4720	568.3
1.695	7258	−3196.9	3.676	6788	463.9	5.581	4734	606.9
1.725	7272	−3108.8	3.706	6696	419.3	5.610	4732	628.8
1.756	7367	−2940.3	3.737	6614	384.0	5.640	4702	623.0
1.787	7415	−2818.0	3.767	6508	325.2	5.669	4698	642.3
1.818	7548	−2611.5	3.797	6416	279.6	5.698	4679	646.4
1.848	7663	−2423.1	3.827	6338	246.9	5.727	4657	648.2
1.879	7790	−2222.9	3.857	6251	204.6	5.757	4637	651.2
1.910	7952	−1987.5	3.887	6161	159.8	5.786	4613	649.9
1.940	6085	−1781.4	3.917	6070	112.7	5.815	4585	644.7
1.971	8211	−1582.5	3.947	5957	43.5	5.844	4524	606.1
2.002	8339	−1382.3	3.978	5884	13.9	5.873	4490	595.0
2.032	8413	−1234.9	4.008	5811	−16.4	5.902	4495	586.0
2.063	8475	−1100.8	4.038	5726	−59.4	5.931	4404	552.7
2.094	8557	−945.7	4.068	5625	−118.9	5.960	4360	530.7
2.124	8610	−821.2	4.098	5541	−160.9	5.989	4317	509.0
2.155	8631	−728.1	4.128	5440	−221.1	6.018	4258	471.6
2.185	8616	−671.4	4.158	5366	−254.5	6.047	4187	422.5
2.216	8619	−596.8	4.188	5260	−320.7	6.149	4027	335.4
2.247	8628	−516.3	4.218	5171	−370.6	6.221	3904	263.8
2.277	8580	−493.5	4.248	5102	−400.0	6.293	3737	146.3
2.308	8559	−443.8	4.278	4995	−468.4	6.365	3627	85.2
2.339	8517	−415.4	4.308	4903	−522.1	6.437	3475	10.9

Table 2. (Continued)

s	$I(s)$	$i(s)$	s	$I(s)$	$i(s)$	s	$I(s)$	$i(s)$
6.509	3327	−76.9	10.849	1676	82.6	14.323	917	−16.2
6.581	3199	−146.9	10.910	1663	85.5	14.368	915	−12.3
6.652	3070	−208.8	10.971	1637	75.4	14.413	904	−17.9
6.724	2971	−261.5	11.031	1618	72.0	14.457	898	−19.1
6.795	2903	−307.7	11.091	1602	71.6	14.502	885	−26.1
6.866	2838	−338.7	11.151	1583	67.7	14.546	882	−24.0
6.937	2804	−357.7	11.211	1566	65.1	14.589	884	−16.7
7.008	2770	−365.0	11.271	1546	60.6	14.633	869	−26.5
7.079	2744	−357.7	11.330	1520	48.7	14.676	870	−20.8
7.149	2719	−343.0	11.389	1502	45.2	14.719	855	−30.4
7.220	2705	−318.3	11.448	1470	26.7	14.762	856	−24.3
7.290	2708	−276.2	11.507	1448	18.5	14.804	842	−33.3
7.361	2705	−241.8	11.565	1423	7.5	14.846	840	−30.8
7.341	2719	−190.8	11.623	1403	0.7	14.888	839	−26.9
7.501	2726	−147.9	11.682	1379	−10.4	14.929	832	−29.5
7.570	2743	−94.8	11.739	1360	−16.1	14.970	829	−28.5
7.640	2753	−49.2	11.797	1334	−29.7	15.011	818	−34.5
7.710	2772	3.9	11.854	1323	−27.6	15.052	818	−29.8
7.779	2784	50.5	11.911	1292	−46.3	15.092	822	−22.0
7.848	2795	95.4	11.968	1282	−44.1	15.132	817	−22.6
7.917	2797	130.2	12.025	1258	−56.0	15.172	813	−22.7
7.986	2796	162.0	12.081	1238	−64.9	15.212	813	−19.1
8.055	2771	169.0	12.138	1224	−66.7	15.251	806	−21.6
8.123	2754	183.9	12.194	1219	−60.6	15.290	806	−17.9
8.192	2722	183.4	12.249	1204	−65.0	15.328	802	−17.4
8.260	2684	175.4	12.305	1187	−69.8	15.367	806	−10.5
8.328	2643	165.3	12.360	1174	−72.1	15.405	803	−9.0
8.396	2602	154.8	12.415	1165	−70.6	15.442	801	−7.7
8.464	2551	133.2	12.470	1163	−62.8	15.480	804	−0.8
8.532	2494	105.3	12.525	1159	−56.3	15.517	801	−0.2
8.599	2455	95.4	12.579	1149	−56.2	15.554	796	−1.8
8.667	2402	69.7	12.633	1149	−46.1	15.590	793	−1.0
8.734	2356	52.1	12.687	1142	−42.4	15.626	784	−6.5
8.801	2319	42.4	12.741	1135	−40.4	15.662	795	7.7
8.868	2263	13.7	12.794	1142	−23.6	15.698	799	14.5
8.934	2223	0.6	12.847	1137	−18.7	15.733	791	10.4
9.001	2185	−11.5	12.900	1139	−8.2	15.768	792	14.4
9.067	2154	−17.1	12.953	1137	−8.8	15.803	786	11.1
9.133	2109	−37.0	13.005	1137	8.4	15.838	787	15.1
9.199	2067	−53.9	13.057	1131	10.6	15.872	785	16.2
9.265	2031	−64.8	13.109	1128	16.8	15.906	779	13.2
9.331	1999	−72.2	13.161	1127	24.4	15.939	777	13.9
9.396	1965	−82.5	13.212	1119	24.4	15.972	777	17.8
9.461	1936	−88.1	13.263	1117	31.4	16.005	773	15.6
9.526	1904	−96.5	13.314	1111	33.3	16.038	766	11.7
9.591	1883	−94.9	13.365	1104	33.9	16.070	765	13.4
9.656	1857	−98.7	13.415	1100	38.3	16.102	759	10.3
9.721	1822	−111.2	13.465	1091	36.7	16.134	763	17.1
9.785	1800	−112.3	13.515	1080	33.8	16.166	759	15.9
9.849	1789	−101.2	13.565	1078	39.6	16.197	755	14.2
9.913	1761	−108.6	13.614	1064	33.2	16.227	756	17.4
9.977	1758	−91.3	13.663	1055	31.4	16.258	753	16.9
10.040	1750	−78.4	13.712	1049	32.4	16.288	752	18.6
10.104	1742	−66.4	13.761	1036	26.4	16.318	744	13.0
10.167	1726	−62.7	13.809	1028	25.0	16.348	740	11.5
10.230	1729	−40.4	13.857	1017	21.4	16.377	739	12.6
10.293	1724	−26.6	13.905	1006	16.6	16.406	738	13.8
10.356	1717	−15.7	13.952	992	9.9	16.434	733	11.1
10.418	1720	6.2	14.000	985	9.2	16.463	725	5.2
10.480	1715	19.0	14.047	969	−1.1	16.491	726	8.6
10.542	1715	36.8	14.093	968	4.5	16.518	717	1.8
10.604	1707	46.5	14.140	957	−0.1	16.546	720	6.8
10.666	1701	57.2	14.186	948	−2.5	16.573	715	3.5
10.727	1702	75.2	14.232	941	−4.7			
10.788	1685	75.1	14.278	937	−2.4			

The measured intensities, $I(s)$, corrected for polarization and normalized to correspond to the stoichiometric unit of volume were used to calculate the reduced intensities, $i(s)$, according to the formula:

$$i(s) = I(s) - \sum_i n_i[(f_i(s)+\Delta f_i')^2+(\Delta f_i'')^2 + \Phi(s)\cdot I_i^{inco}(s)] \quad (1)$$

Here $s=4\pi\sin\theta/\lambda$, n_i represents the number of atoms "i" in the stoichiometric unit of volume, f_i is the scattering factor, $\Delta f_i'$ and $\Delta f_i''$ are the real and the imaginary parts of the anomalous dispersion correction, $\Phi(s)$ is the fraction of the incoherent radiation reaching the counter, and $I_i^{inco}(s)$ is the total incoherent radiation of an atom "i".

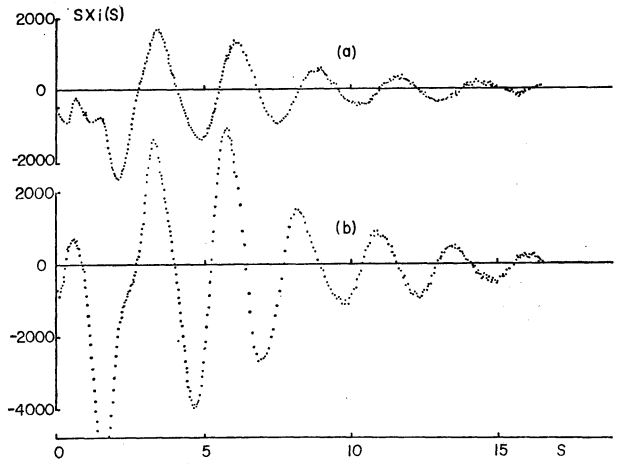

Fig. 1. Observed $s\cdot i(s)$ values for the chloride and the bromide solutions given as a function of $s=4\pi\sin\theta/\lambda$

The reduced intensities, $i(s)$, multiplied by s are shown in Fig. 1 and in Table 2. From these values, the radial distribution curves, $D(r)$, were calculated according to the expression:

$$D(r) = 4\pi r^2\rho_0 + 2r\pi^{-1}\int_0^{s_{max}} s\cdot i(s)\cdot M(s)\cdot\sin(rs)ds \quad (2)$$

where ρ_0 denotes the average scattering density of the sample in electron units. The modification function, $M(s)$, was chosen to be $(f_{Au}^2(0)/f_{Au}^2(s))\exp(-0.01s^2)$. Spurious peaks below 1 Å in the distribution functions, which could not correspond to interatomic distances, were used to correct the reduced intensity curves for low-frequency additions.

Theoretical intensities due to interatomic interactions were calculated from Eq. (3).

$$i(s) = \sum_i\sum_j f_i(s)f_j(s)\frac{\sin(r_{ij}s)}{r_{ij}s}\exp(-b_{ij}s^2) \quad (3)$$

where r_{ij} is the distance between two atoms "i" and "j", $f_i(s)$ and $f_j(s)$ are the scattering factors, and b_{ij} is the temperature factor corresponding to the interaction between the "i" and "j" atoms.

All calculations were carried out with the use of the KURVLR program.[19]

Analysis of the Intensity Data

The intensity data were first analyzed by means of the radial distribution functions (Fig. 2) calculated

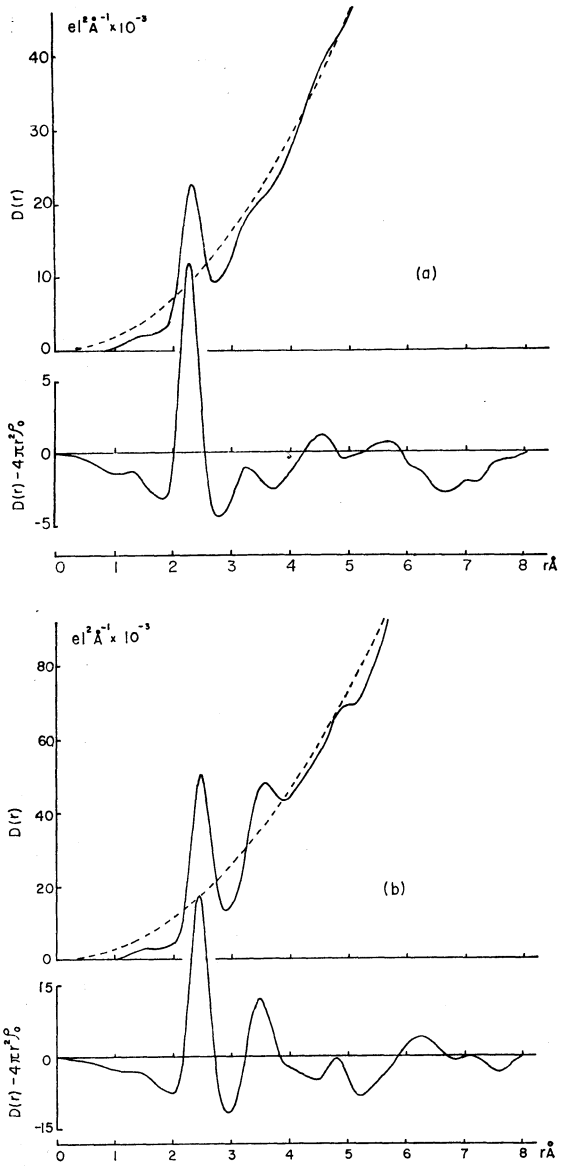

Fig. 2. Radial distribution curves, $D(r)$ and $D(r)-4\pi r^2\rho_0$
(a) The chloride solution. (b) The bromide solution

according to Eq. (2). Distances of gold-halogen and halogen-halogen atoms within a complex were determined from the corresponding peak positions in the distribution functions. The number of such interactions could be roughly estimated from the areas under the peaks.

The first pronounced peak in the radial distribution function (RDF) occurs at 2.3 Å for the chloride solution and 2.4_5 Å for the bromide solution. These peaks can be identified as corresponding to Au–Cl and Au–Br distances within the complexes, since in crystal structure determinations of $KAuCl_4$[6] and of $AuCl_3$,[5] for example, the Au–Cl distances within the planar $AuCl_4^-$ complexes have been found to be around 2.3 Å. Two more pronounced peaks occur in the RDF for the bromide solution: at 3.4 Å ($\simeq\sqrt{2}\times 2.45$ Å) and 4.9 Å ($=2\times 2.45$ Å). Corresponding peaks are present also for the chloride solution but are relatively much smaller.

These two peaks can be identified as Br–Br or Cl–Cl interactions. They occur at distances expected for a planar $AuBr_4^-$ or $AuCl_4^-$ complex. No other marked peaks, which can be related to intramolecular interactions, are present in the RDF functions. The RDF-s therefore are consistent with a square planar symmetry for the $AuCl_4^-$ and the $AuBr_4^-$ complexes.

Refinement of the Structures

In order to get more precise values for the structures of the complexes the influence of intermolecular interactions must be estimated or eliminated. This was done by adjusting the parameter values, derived from the RDF-functions, by means of a least squares procedure in which a minimum was sought for the function

$$\sum_{s_{min}}^{s_{max}} w(s)[i(s)_{obs}-i(s)_{calc}]^2.$$

Intermolecular interactions give their largest contributions to the reduced intensities, $i(s)$, at low s values, while intramolecular interactions are the main contributors at the larger s values. With only intramolecular interactions included for $i(s)_{calc}$ it was found that when the least squares refinements were carried out for different values of s_{min} the resulting parameter values did not show any systematic variations with the chosen s_{min} value for $s_{min}>2.5$ Å^{-1}. It was concluded, therefore, that the intermolecular interactions had a negligible influence on the results, if $i(s)$ values for $s<2.5$ Å^{-1} were excluded from the refinements. Consequently only intensity values for $2.6<s<16.5$ were used for the subsequent least-squares refinements.

The weighting factors, $w(s)$, were chosen to give approximately equal contributions to the least-squares error sum from each experimental $i(s)$ value. For each intramolecular interaction included for the calculation of $i(s)_{calc}$ three parameter values could be refined: the distance, r_{ij}, the temperature factor, b_{ij} and a frequency factor, n_{ij}. Various restrictions on the allowed variations of the values of the parameters could be imposed in the calculations in order to retain a given symmetry during a refinement.

Table 3 summarizes the results of four different types of refinements referred to by A, B, C, and D.

A. Only Au–Cl or Au–Br interactions were included for $i(s)_{calc}$. The distance, the temperature factor and the frequency factor were refined.

B. In this refinement, which could be carried out only for the bromide solution, the Au–Br and the Br–Br interactions were refined independently. The bromide atoms were assumed to be arranged in a square, the size of which was varied in the refinement.

C. The $AuCl_4^-$ and the $AuBr_4^-$ complexes were assumed to form planar squares with the Au atom at the center of the square. The gold-halide distance, the corresponding temperature factor and a temperature factor for the halide-halide interactions were refined.

D. In addition to the parameters used in the previous refinement the concentration of the complexes was varied.

As shown by the results in Table 3 the different restrictions imposed on the refinements do not lead to any significant differences in the resulting parameter values. The independent refinement of the Au–Br and the Br–Br interactions in (B) leads to a ratio between these distances of $3.44/2.431=1.41$ which is close to the expected value of $\sqrt{2}=1.414$ for a square planar complex. In addition the number of Au–Br and of Br–Br interactions per Au atom does not differ significantly from the value of four expected for a AuX_4^- complex. The refinement of the concentration of the AuX_4^- complex in D does not lead to any significant difference from the analytically determined concentration of gold in the solution (Table 1), which indicates that all gold is bonded in AuX_4^- complexes.

Table 3. Summary of the results of the least-squares refinements

	$AuCl_4^-$	$AuBr_4^-$
A.	$r_{Au-Cl}=2.288[2]$Å	$r_{Au-Br}=2.422[4]$Å
	$b_{Au-Cl}=0.0011[4]$Å^2	$b_{Au-Br}=0.0016[6]$Å^2
	$n_{Au-Cl}=3.5[2]$	$n_{Au-Br}=4.0[2]$
B.		$r_{Au-Br}=2.431[3]$Å
		$b_{Au-Br}=0.0012[3]$Å^2
		$n_{Au-Br}=3.9[1]$
		$r_{Br-Br}=3.44[1]$Å
		$b_{Br-Br}=0.003[1]$Å^2
		$n_{Br-Br}=4.1[2]$
C.	$r_{Au-Cl}=2.291[2]$Å	$r_{Au-Br}=2.432[3]$Å
	$b_{Au-Cl}=0.003[2]$Å^2	$b_{Au-Br}=0.0017[10]$Å^2
	$b_{Cl-Cl}=0.004[2]$Å^2	$b_{Br-Br}=0.006[2]$Å^2
D.	conc.$=2.8[1]$M	conc.$=2.72[5]$M
	$(=90[4]\%)$	$(=98[2]\%)$
	$r_{Au-Cl}=2.291[2]$Å	$r_{Au-Br}=2.433[2]$Å
	$b_{Au-Cl}=0.002[2]$Å^2	$b_{Au-Br}=0.0012[5]$Å^2
	$b_{Cl-Cl}=0.002[2]$Å^2	$b_{Br-Br}=0.006[1]$Å^2

Table 4. Final parameter values from the least-squares refinements

$AuCl_4^-$	$AuBr_4^-$
$r_{Au-Cl}=2.291[3]$Å	$r_{Au-Br}=2.432[3]$Å
$b_{Au-Cl}=0.002[2]$Å^2	$b_{Au-Br}=0.0012[5]$Å^2
$b_{Cl-Cl}=0.003[2]$Å^2	$b_{Br-Br}=0.006[2]$Å^2
$n_{Au-Cl}=3.6[2]$	$n_{Au-Br}=3.9[1]$

The best parameter values and the corresponding standard deviations are given in Table 4. The standard deviations are those calculated in the least-squares refinements and do not include possible systematic errors. As judged from the agreement between results obtained when intensities from different s ranges were used for the refinements such systematic errors are probably small and do not exceed the given standard deviations.

To check the calculations the parameter values given in Table 4 were used to calculate peak shapes for the intramolecular interactions. These are compared in Fig. 3 with the radial distribution curves. Subtraction of the calculated peaks from these curves leads to smooth background curves with no indications of residual intramolecular interactions. The $s\cdot i(s)_{calc}$ values are compared in Fig. 4 with the $s\cdot i(s)_{calc}$ values. The differences between observed and calculated values shown in the same figure show that the complexes

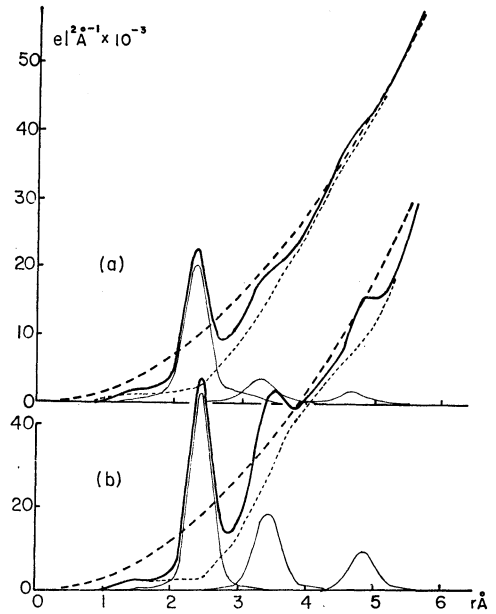

Fig. 3. Comparison between radial distribution curves and peak shapes calculated for the interactions in the AuX_4^- ions using the parameters in Table 4. The difference between the distribution curve and the calculated peaks is shown by the dashed line.
(a) The chloride solution. (b) The bromide solution.

assumed are sufficient to reproduce the observed intensities except for s values below about 3 $Å^{-1}$, where intermolecular interactions can be expected to become important.

The Au–Cl and the Au–Br distances found here for the complexes in solution (Table 4) are similar to those found in crystals in which $AuCl_4^-$ and $AuBr_4^-$ ions have a planar configuration. In crystals of $Cs_2AgAuCl_6$[3] and $RuAuCl_4$[5] the Au–Cl distances have been reported to be about 2.30 and 2.28 Å, respectively. Somewhat longer distances, 2.42 Å, have been reported for crystals of $Cs_2AuAuCl_6$.[3] Other values for the distances ranging from 2.20 to 2.37 Å with an average value of 2.28_6 Å have been found in $KAuCl_4$.[6] Values ranging from 2.25 to 2.34 Å, with an average value of 2.29_0 Å, have been found in crystals of $AuCl_3$, which contain the dimer Au_2Cl_6.

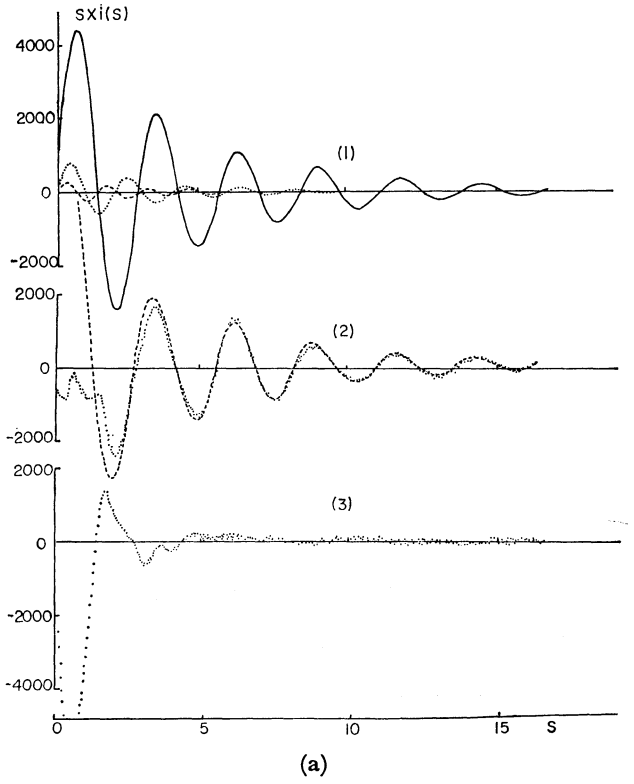

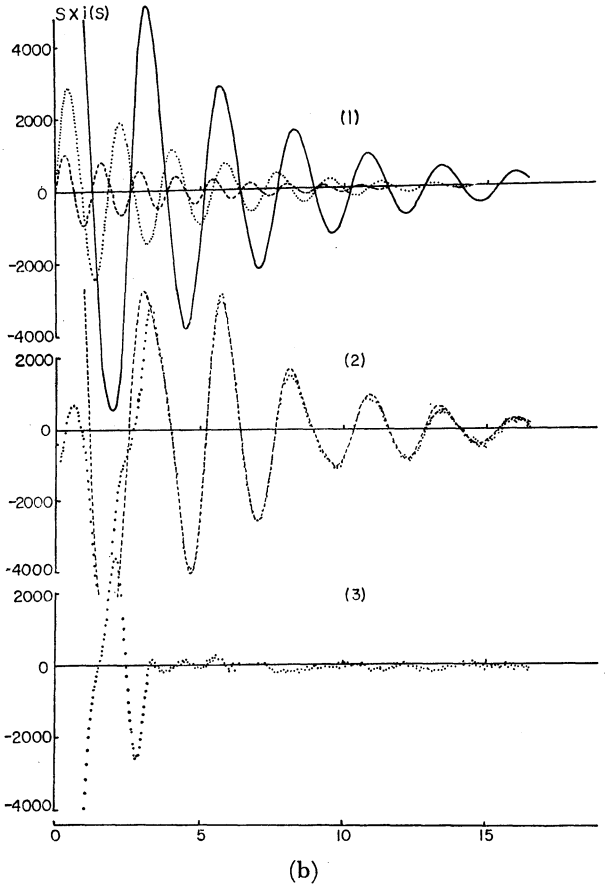

Fig. 4. Observed and calculated $s \cdot i(s)$ values for the chloride solution (a) and the bromide solution (b).
(1) Calculated $s \cdot i(s)$ values for the interactions within an AuX_4^- ion: Au–X full drawn line, *cis*-X–X dotted line and *trans*-X–X dashed line.
(2) Comparison between observed $s \cdot i(s)$ value (dots) and calculated $s \cdot i(s)$ values (dashed line).
(3) Difference between observed and calculated $s \cdot i(s)$ values.

The temperature factors found for the complexes in solution are small and correspond to root mean square values for the variations of the distances of about 0.02 Å for the gold-halide and about 0.03 Å for the halide-halide distances. This indicates a regular arrangement of the atoms in the complexes with no structural differencies between the distances.

This work was carried out at the Institute of Technology in Stockholm and was supported by the Swedish Natural Science Research Council. Computer time was made available by the Computer Division of the National Swedish Office for Administrative Rationaliza-

tion and Economy. We thank Dr. Derek Lewis for revising the English text.

References

1) L. G. Sillén and A. E. Martell, Stability Constants, Spec. Publ. No. 17 and Supplement No. 1, Spec. Publ. No. 25, The Chemical Society, London, 1964 and 1971.
2) H. Stammreich and R. Forneris, *Spectrochim. Acta*, **16**, 363 (1960).
3) N. Elliott and L. Pauling, *J. Amer. Chem. Soc.*, **60**, 1846 (1938).
4) E. G. Cox and K. C. Webster, *J. Chem. Soc.*, **1936**, 1635.
5) J. Strähle and H. Bärninghausen, *Z. Naturforsch.*, *B*, **25**, 1186 (1970).
6) M. Bonamico and G. Dessy, *Acta Crystallogr.*, **B29**, 1735 (1973).
7) D. M. Adams and H. A. Gebbie, *Spectrochim. Acta*, **19**, 925 (1963).
8) A. Sabatini, L. Sacconi, and V. Schettino, *Inorg. Chem.*, **3**, 1775 (1964).
9) G. Johansson, *Acta Chem. Scand.*, **20**, 553 (1966).
10) F. Gaizer and G. Johansson, *ibid.*, **22**, 3013 (1968).
11) N. Norman, *Acta Crystallogr.*, **10**, 370 (1957).
12) J. Krogh-Moe, *ibid.*, **9**, 951 (1956).
13) D. T. Cromer and J. T. Waber, *ibid.*, **18**, 104 (1965).
14) R. F. Stewart, E. K. Davidson, and W. T. Simpson, *J. Chem. Phys.*, **42**, 3175 (1965).
15) D. T. Cromer and J. B. Mann, *ibid.*, **47**, 1892 (1967).
16) D. T. Cromer, *ibid.*, **50**, 4857 (1969).
17) A. H. Compton and S. K. Allison, "X-Rays in Theory and Experiment," van Nostrand, New York (1935).
18) D. T. Cromer and D. Lieberman, *J. Chem. Phys.*, **53**, 1891 (1970).
19) G. Johansson and M. Sandström, *Chemica Scripta*, **4**, 195 (1973).